Neuroscience 155 (2008) 277–282

HIGH-FIDELITY EVOKED POTENTIAL FOR MAPPING THE RAT TAIL IN THALAMUS

F.-S. JAW,* Y.-C. KAO, C.-P. CHEN, C.-Y. LEE AND Y.-Y. CHEN

Institute of Biomedical Engineering, National Taiwan University, No. 1, Sec. 4, Roosevelt Road, Taipei, Taiwan, R.O.C. 10617

Abstract—The technique of field potentials (FPs) provides a macroscopic view for exploring brain function, and is supplementary to single-unit recording, a microscopic view that investigates each neuron in great detail. Mapping the rat tail in the ventroposterolateral (VPL) nucleus of the thalamus was carried out by analyzing the current source density (CSD) of the evoked FPs. The results showed a clear somatotopic organization of the tail in the VPL nucleus. Also, to obtain high-fidelity FPs, two recording parameters were determined. Based upon cross-correlation coefficient (ρ), the cycles of FPs needed to be averaged should not be less than 50 and the distance between the two recording sites should be no longer than 50 μm in each direction (mediolateral, anteroposterior and ventrodorsal). Under these conditions, the representation (or reproducibility) of an FP can be >95%. The procedures used to determine these parameters can serve as a guide to obtain FPs with high signal-to-noise ratio and without spatial aliasing error.

Key words: evoked potential, current source density, rat thalamus, A_β fibers, correlation coefficient, signal average.

The brain contains billions of neurons that function simultaneously in parallel, hence, the electrical signals in the CNS are very complex. Therefore, it is helpful to choose a simpler system as a model. Barrel organization in the rat cerebral cortex is a well-established model for studying the tactility of whiskers (Arabzadeh et al., 2004; Kublik, 2004; Woosley and Ven Der Loos, 1970). However, it is probably not an adequate model for nociceptive experiments, because we do not know how to apply painful stimuli to whiskers. The rat tail, as compared with whiskers, is very long and simple, and has plenty of room for applying various stimuli, such as touch, pinching, laser (Shaw et al., 2001), as well as electric shock (Shyu et al., 2003). Furthermore, its representation in the CNS is very small, thus enabling us to map it systematically and thoroughly with limited manpower. As a result, this study was designed to map in the thalamus the responses produced by stimulating the A_β fibers of the rat tail.

Single-unit recording (Chung et al., 1986; Zhang and Giesler, 2005) is widely used in electrophysiological research. This method is able to investigate the characteristics of each individual neuron. It is, however, difficult to record several neuronal signals simultaneously from different locations (Dong et al., 1982; Buzsaki et al., 1989). As compared with the microcosmic information of single-unit recording, the technique of field potentials (FPs) offers macrocosmic information (Chudler and Dong, 1983). FPs are generated by integral electrical signals that compromise the activities of many neurons, conducted via the large volume of the extracellular space. Hence, information about FPs can be used to observe the activities of a group of neurons.

Current source density (CSD) analysis of FPs can tell the location at which post-synaptic potentials occur, so the changes in time and location of neuronal activities can be established. Before the analysis of FPs, we investigated the criteria for FPs recording. The purpose of doing this was to record high-quality signals. Cross-correlation coefficient was used as an objective index to evaluate the adequacy of signal averaging and the necessary spatial density of the FPs. It is suggested from our results that the spatial interval between two recording points should be shorter than 50 μm and 50 cycles of FPs should be averaged to obtain 95% confidence intervals. Finally, the CSD showed that there was a good somatotopic organization of the rat tail in the ventroposterolateral (VPL) nucleus of the thalamus.

EXPERIMENTAL PROCEDURES

Animal preparation

Adult male Wistar rats, weighing 350–450 g, were used. All experiments were carried out in accordance with the guidelines of the National Taiwan University College of Medicine and College of Public Health Institutional Animal Care and Use Committee (IACUC), as well as the National Institutes of Health Guide for the Care and Use of Laboratory Animals (NIH Publications No. 80-23). All efforts were made to minimize the number of animal used and their suffering. After anesthesia with sodium pentobarbital (50 mg/kg, i.p.), the trachea, femoral artery and femoral vein were cannulated. The adequacy of anesthesia was maintained by continuous delivery of pentobarbital with an infusion pump at a lower dosage (5 mg/mL, 1 mL/h, i.v.). Rectal temperature was maintained at 38 °C with an electrical thermal blanket. The animals were placed on the stereotaxic apparatus (Spinal Unit of David Kopf) for recording. Before systematic recording was performed, we lightly tapped the tail of the rat with a glass rod to determine the responsive regions in the thalamus, with the aid of an audio monitor (Moncastle and Henneman, 1952). A total of five rats were used in this experiment to map the tail in the thalamus at various coronary planes (Fig. 1). This procedure speeded up the determination of the area of the thalamus where we should record.

*Corresponding author. Tel: +886-2-23687401; fax: +886-2-33665268.
E-mail address: jaw@ntu.edu.tw (F.-S. Jaw).

Abbreviations: CSD, current source density; EPSP, excitatory postsynaptic potential; FP, field potential; S/N, signal-to-noise; VPL, ventroposterolateral; ρ, function of correlation coefficient.

0306-4522/08$32.00+0.00
doi:10.1016/j.neuroscience.2008.05.034

Thereafter, laminectomy (from L_1 to S_2) and craniotomy were performed, the animals were paralyzed with gallamine triethiodide (2%) to depress the reflex response, and were artificially ventilated (Harvard 683; 10 mL/kg, 1 Hz). Both the dura maters of the brain and spinal cord were carefully removed by microscopic dissection. The exposed brain and spinal cord were covered with warm liquid paraffin (34 °C) in the oil pool formed with the cut skin. During the experiment, the animals were kept under physiological conditions (mean blood pressure >90 mm Hg, end tidal CO_2 concentration 3–4.5%, and rectal temperature 38 °C).

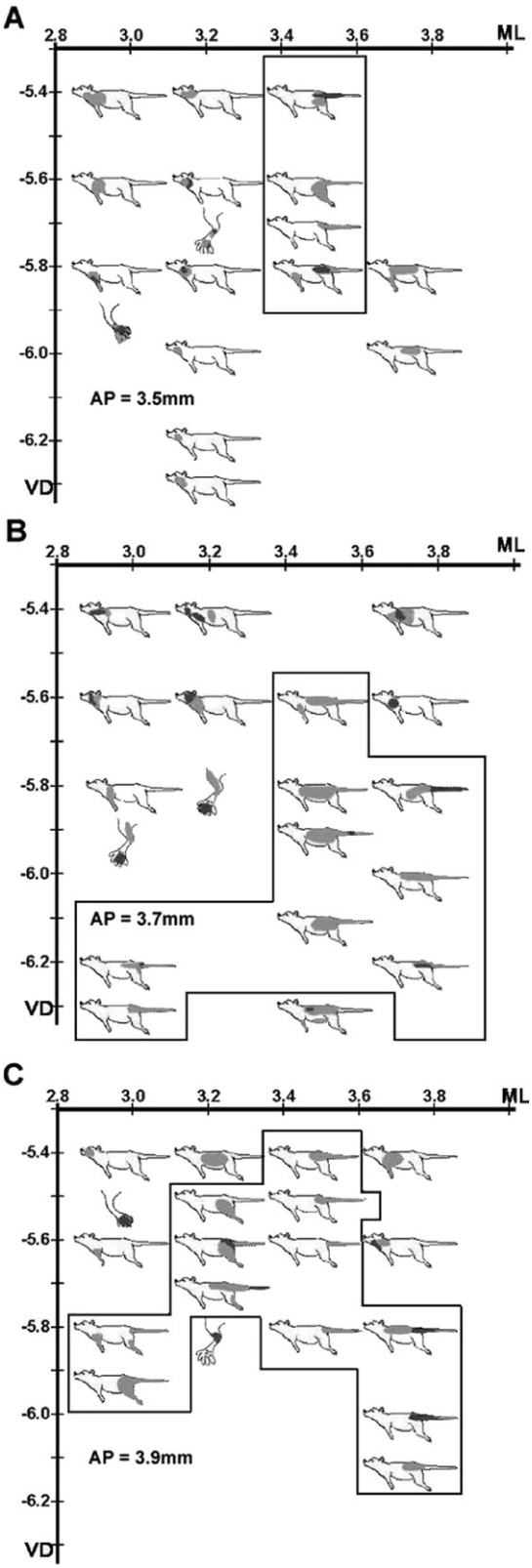

Recording setup

Glass micropipettes with a large-tip diameter (Briano, 1983) were filled with 3 M NaCl solution. Thus, the impedance could be decreased to 3–5 MΩ for noise reduction. The FPs picked up were amplified with a gain of 2500, filtered with a passband from 0.01–300 Hz, and digitized at 3000 Hz by an A/D converter card (NI PCI-MIO-16E-4). Also, an audio monitor (Grass AM8) and an oscilloscope (Tektronix TDS 520A) were used for locating the responsive areas in the thalamus.

The tail of the rat was primary innervated by the S_2, S_3 and S_4 roots (Lee, 1991). Therefore, these roots were dissected with fine glass rods, cut distally, and hooked individually on multi-lead hook electrodes for recording and stimulation. A 1-Hz constant current pulse with a duration of 100 μs was used to elicit supramaximally the A_β fibers of these roots. The supramaximal stimulus was defined as 1.5 times the intensity of stimulus that elicits maximal A_β compound action potentials (CAPs).

To confirm the recording site, three rats were killed with the tip of the electrode left *in situ* after recording. Then, transcardiac perfusion was performed with buffered formaldehyde (10%). After about 1 week post-fixation, the rat brains were cryosectioned at 50 μm thickness and Nissl stained. Consecutive sections were examined to locate the tip of the glass microelectrode.

Determination of recording parameters

Two important recording parameters should be determined at the first step. One is the number of cycles for averaging, and the other is the spatial interval between two consecutive recording points. Signal averaging is a technology commonly used for increasing the signal-to-noise (S/N) ratio of evoked potentials. However, how many cycles should be averaged lacks objective guidance. To set up the guidance, we determined these two parameters, based on correlation function, which quantitatively measures the similarity between two signals (Goovaerts and Rompelman, 1991).

In general, the function of correlation coefficient (ρ) can be formulated as follows (Freeman and Nicholson, 1975):

$$\rho = \frac{\sum (x-\mu_x)(y-\mu_y)}{\sqrt{\sum (x-\mu_x)^2 \sum (y-\mu_y)^2}} = \frac{E(xy)-\mu_x\mu_y}{\sigma_x\sigma_y}, \quad (1)$$

where μ and σ represent, respectively, the mean and standard deviation of the signal.

By using ρ, one can find the effect of the number of cycles used for signal averaging, and the effect of changing the spatial sampling interval. For compliance with statistical convention, 95% of ρ was selected as the minimal acceptable level of confidence.

Fig. 1. Somatotopic organization in the VPL nucleus of the rat thalamus. Each receptive field is denoted in the corresponding position, which indicates the site where neuronal activity was evoked by touch. (A–C) Coronal planes at 3.5, 3.7 and 3.9 mm posterior to the bregma, respectively. The range covers 2.8–3.8 mm mediolaterally and 5.3–6.3 mm in depth.

CSD analysis

Analysis of CSD provides information about ions moving in or out of the cell membrane. The place where ions move into neuronal membranes is called “sink” for an excitatory postsynaptic potential (EPSP) On the other hand, “source” refers to the place where ions flow out of neuronal membranes. The gathered data were then analyzed with a MATLAB program to calculate the CSD profile.

The relationship between FP and its CSD is described by a Poisson equation as follows:

$$\nabla \bar{J} = -I_V = -\sigma \nabla^2 \phi, \tag{2}$$

where σ is the conductivity of the conducting medium and ϕ the FP.

The three-dimensional expression of Eq. 2 in cartesian coordinates is:

$$\sigma_x \frac{\partial^2}{\partial x^2}\phi + \sigma_y \frac{\partial^2}{\partial y^2}\phi + \sigma_z \frac{\partial^2}{\partial z^2}\phi = -I_v, \tag{3}$$

where σ_x, σ_y, and σ_z are the conductivities of the three axes.

If the recording area is small, the tissue conductivities along all of the axes can be assumed to be homogeneous, especially at the VPL nucleus (Mcallister and Willis, 1981). Then, Eq. 3 can be simplified to the following relationship:

$$-I_v \alpha \left(\frac{\partial^2}{\partial x^2}\phi + \frac{\partial^2}{\partial y^2}\phi + \frac{\partial^2}{\partial z^2}\phi \right) \tag{4}$$

Their finite difference equivalences can be obtained thereafter:

$$CSD_x \approx \frac{\phi(t, x+\Delta x) - 2\phi(t, x) + \phi(t, x-\Delta x)}{\Delta x^2} \tag{5}$$

$$CSD_y \approx \frac{\phi(t, y+\Delta y) - 2\phi(t, y) + \phi(t, y-\Delta y)}{\Delta y^2} \tag{6}$$

$$CSD_z \approx \frac{\phi(t, z+\Delta z) - 2\phi(t, z) + \phi(t, z-\Delta z)}{\Delta z^2} \tag{7}$$

$$I_v = -\left(CSD_x + CSD_y + CSD_z\right), \tag{8}$$

where Δx, Δy, and Δz are the spatial interval of adjacent recording sites in the ML, AP, and VD directions.

RESULTS

Tactile mapping of the tail

Before FP recording, somatotopic organization of the rat thalamus has to be mapped. The responses detected by the aid of the audio-monitor are shown in Fig. 1. Three coronal planes are shown. Only few recording points could be found on the 3.5-mm plane. The responsive points clustered on the 3.7- and 3.9-mm planes were broader and deeper than those on the 3.5-mm plane. The peripheral receptive fields of the recording sites were hatched in the rat cartoon.

Number of cycles to be averaged and spatial interval for recording

Firstly, the number of cycles to be averaged had to be determined to obtain the representative response at the recording point. Three pairs of the evoked responses are shown in Fig. 2A. The fastest component conveyed by the A_β fibers was at ~12.5 ms, which was indicated by the dashed line. The number of cycles used for averaging and their corresponding ρ were shown in Fig. 2A. The resultant waveforms suggested that the larger the number of cycles averaged, the higher ρ was. To inspect the trend between

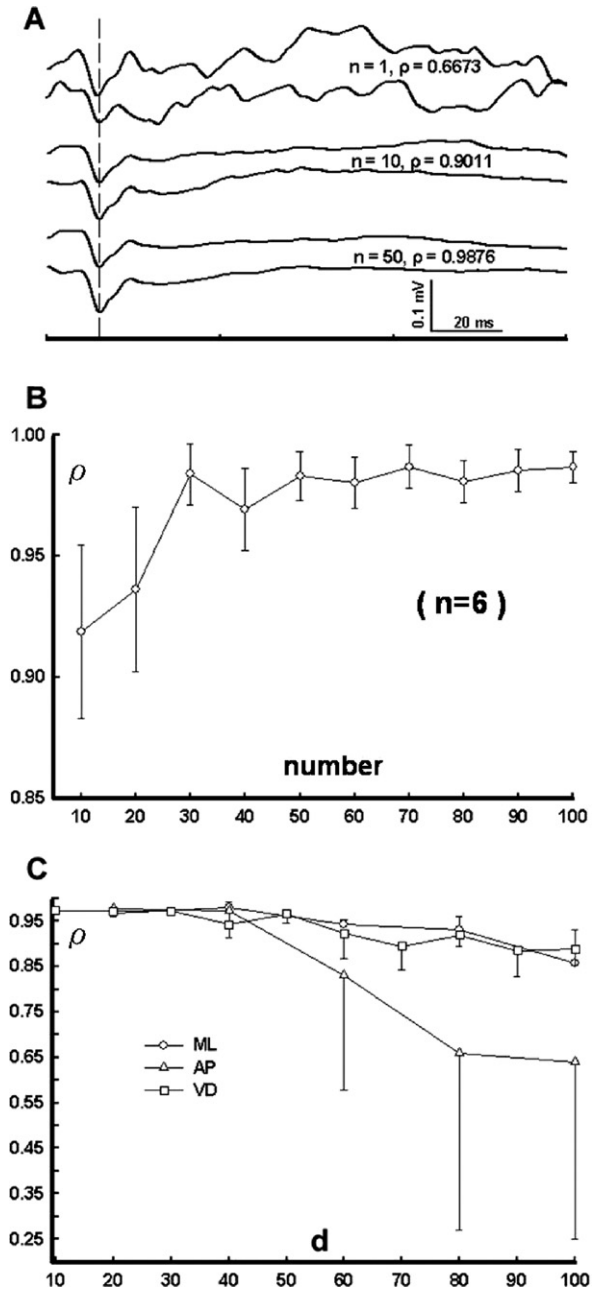

Fig. 2. Determination of parameters for FP recording. (A) The effect of different number of averaging on FP waveform. In all three pairs of waveforms, *n* represents the number of average, while ρ is the cross-correlation coefficient of two waveforms. Averaging 50 responses yielded a good S/N ration, with $\rho > 95\%$. The trend of ρ vs. the number of averaging is depicted in (B). As shown in (C), at a 10-μm interval ρ reached 0.99, and it decreased to 0.95 as the interval increased to of 50 μm. It is even smaller than 0.95, if the interval between two consecutive recording points in the ML and VD directions is >60 μm and >50 μm in the AP direction. (This figure has been used previously to determine the inter-electrode distance of our neuroprobe Chen et al., 2004).

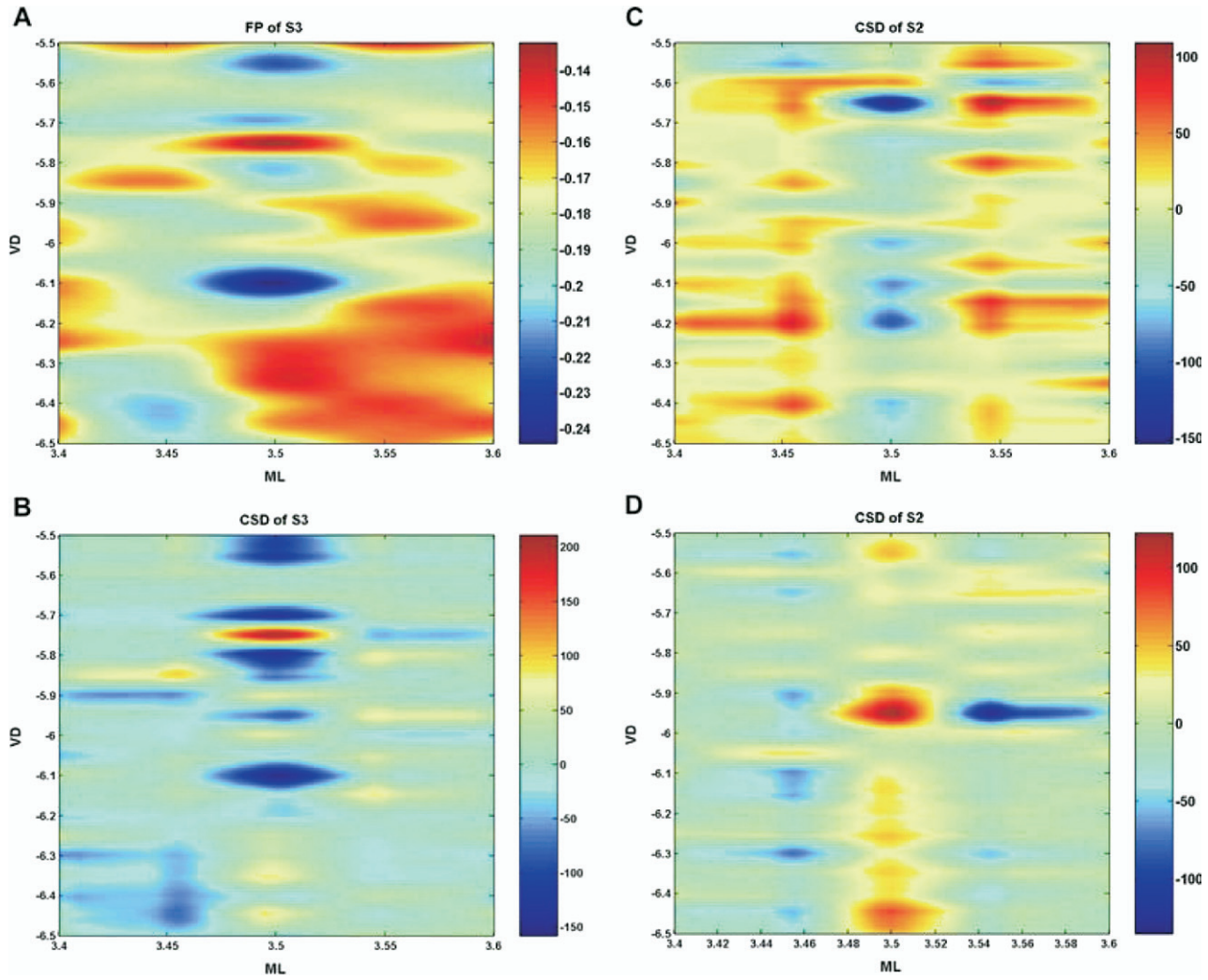

Fig. 3. CSD analysis of FPs evoked from different dorsal roots. (A) The two-dimensional FP was plotted at 12.5 ms, the fastest response evoked by the S_3 root (AP, 3.5 mm). Its CSD analysis is shown in (B). Current sinks (blue) correspond to positive ions entering neurons, as would happen in an EPSP. Current sources (red) are the current that must flow out of the neurons in order to balance the movement of ions. The CSD in different coronal planes induced by stimulating the S_2 root is shown in (C) (AP, 3.5 mm) and (D) (AP, 3.7 mm).

ρ and this number, Fig. 2B was plotted. It was clear that, while this number was >50, ρ would be $>95\%$, with a small variation. Thus, 50 cycles of responses were gathered at each recording site for further analysis.

The other important parameter was concerned with the spatial resolutions in the ML, AP, and VD directions. Also, the correlation coefficient ρ is used for determining whether a spatial interval is too long and will cause aliasing errors (Jaw, 2001). A three-axis manipulator (David Kopf 1460) with a 10-μm resolution along each axis was used in this experiment. From Fig. 2C, we know that spatial interval along each axis should be <50 μm, to prevent degradation of ρ (i.e. $\rho<95\%$).

CSD of the response

After the area in the thalamus involved with tactile sensation and the recording criteria had been determined, electric stimuli were used for mapping the A_β-fiber responses. For ease of comparison, the 3.5-mm plane was chosen because the tactile responses on this plane were well restricted. The FP and its CSD evoked by the A_β fibers of the S_3 root were shown in Fig. 3A and 3B, respectively. The CSDs caused by stimulating A_β fibers of the S_2 root are shown in Fig. 3C (3.5-mm plane) and 3D (3.7-mm plane).

DISCUSSION

The tactile responses of the tail located in the VPL nucleus of the thalamus were confirmed by histological examination (see Fig. 4) and by checking with an atlas of the rat's brain (Paxinos and Watson, 1998). Generally, the spatial distribution of the rat tail in the thalamus was almost perpendicular to the top surface of the cerebral cortex and was slightly curved along the boundary of the VPL nucleus. The deeper or lower portion of the VPL nucleus displayed the forelimb representation. Posterior to the plane of

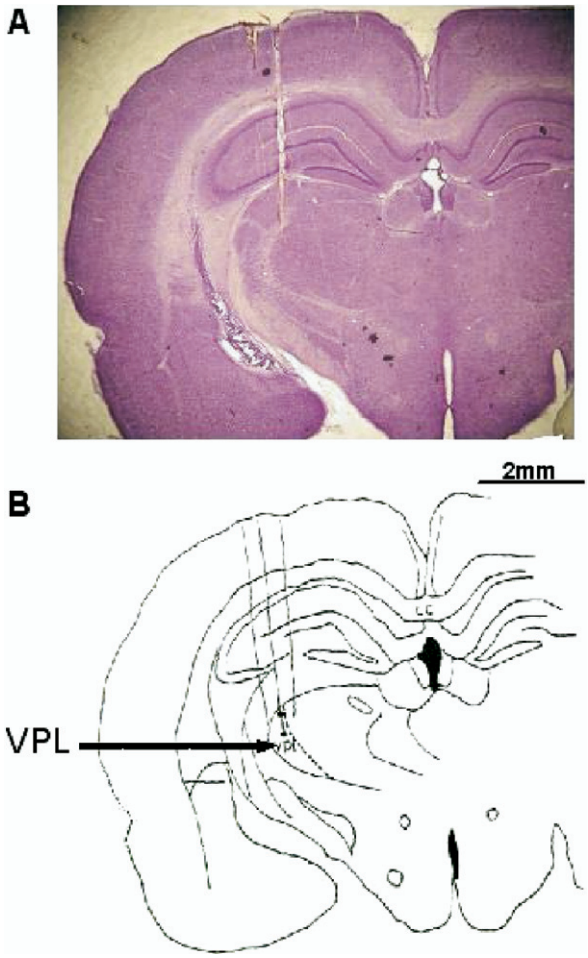

Fig. 4. Histological examination of the recording site. (A) Nissl staining of the slice shows the tip of the glass microelectrode, and (B) is its drawing made with the camera lucida. Three consecutive slices of 50 μm thickness were superimposed to make this drawing, which shows three traces of penetration.

3.5 mm (from the bregma), the receptive fields of the tail showed bifurcation; one part was located in the more ventromedial region, while the other was more lateral. The former may project to the S_2 region and the latter to the S1 region of the cerebral cortex (Davidson, 1965). All these functional topographic findings confirm with the previous studies while placing special emphasis on the mapping of the tail that is not yet clearly understood.

The number of cycles of FPs used for signal averaging does not have clear guidelines for its selection, despite the wide acceptance of this technique for increasing the S/N ratio. On scientific (or mathematical) merit, the correlation coefficient function was used for determining this number. The relationship between this number (n) and ρ shown Fig. 2B suggested that an adequate number for n was 50. This number may intuitively depend on the environmental conditions. A noisy environment may require more cycles to be recorded for averaging. Conversely, a properly grounded and shielded recording setup may need fewer cycles to be measured. Also, the depth of anesthesia of the animals plays a key role in background fluctuation of FPs. Hence, adequate anesthesia is a prerequisite for establishing the number needed for averaging.

The correlation function was also used for determining the sampling distance (d) between two consecutive recording points. From Fig. 2C, the value of ρ decreased below 0.95 if d was >60 μm, especially in the AP direction. This interesting phenomenon may be due to orientation of the medial lemniscus. Thus, a small increment in this direction may cause a large variation in the FPs recorded. This is why the sampling interval in the AP direction will determine the spatial density for the three-dimensional recording.

Systematic mapping of the A_β-fiber response could be carried out only after the recording parameters and extent of the response had been determined. In contrast of FP, which seems confusing because ionic movements (instead of potentials) are the actual cause of activity in living tissue, CSD results could reveal the responsive region clearly and consistently. By comparing Fig. 3B, C and D, one could ascertain that the tail clearly showed somatotopic organization in the thalamus. The responsive center of the S_3 root was at the 3.5-mm coronal plane (Fig. 3B), while that of the S_2 root was at the 3.7-mm plane (Fig. 3D). Somatotopic organization of the tail was not only shown in the AP, but also in the VD direction. The center of the S_3 root was at a depth of 5.75 mm, measured from the surface of the cortex, and that of the S_2 root was at 5.95 mm. Recordings from other rats or from the S_4 roots also supported this finding (data not shown).

CONCLUSION

In summary, CSD analysis rather than FP can be used to display actual active centers of tactile applied on the rat. And there is clear somatotopic organization in the VPL nucleus. The representation of the rat tail in the thalamus, examined for both tactile and electrical stimulation, is relatively small. The recording criteria may vary depending on different conditions, such as environmental noise level and the nature of the signal. However, the method and procedure used to determine these recording parameters in the study provide useful guidance for other applications.

Acknowledgments—This study was supported by 94-EC-17-A-05-S1-017.

REFERENCES

Arabzadeh E, Panzeri S, Diamond ME (2004) Whisker vibration information carried by rat barrel cortex neurons. J Neurosci 24:6011–6020.

Briano RA Jr (1983) A reproducible technique for breaking glass micropipettes over a wide range of tip diameters. J Neurosci Methods 9:31–34.

Buzsaki G, Bickford RG, Ryan LJ, Young S, Prohaska O, Mandel RJ, Gage FH (1989) Multisite recording of brain field potentials and unit activity in freely moving rats. J Neurosci Methods 28:209–217.

Chen YY, Kuo TS, Jaw FS (2004) A laser micromachined probe for recording multiple field potentials in the thalamus. J Neurosci Methods 139:99–109.

Chudler EH, Dong WK (1983) The assessment of pain by cerebral evoked potentials. Pain 16:221–244.

Chung JM, Lee KH, Surmeier DJ, Sorkin LS, Kim J, Willis WD (1986) Response characteristics of neurons in the ventral posterior lateral nucleus of the monkey thalamus. J Neurophysiol 56:370–390.

Davidson N (1965) The projection of afferent pathways on the thalamus of rat. J Comp Neurol 124:377–390.

Dong WK, Harkins SW, Ashleman BT (1982) Origins of cat somatosensory far-field and early near-field evoked potentials. Electroencephalogr Clin Neurophysiol 53:143–165.

Freeman JA, Nicholson C (1975) Experimental optimization of current source-density technique for anuran cerebellum. J Neurophysiol 38:369–382.

Goovaerts HG, Rompelman O (1991) Coherent average technique: a tutorial review. J Biomed Eng 13:275–280.

Jaw FS (2001) Optimal sampling of electrophysiological signals. Neurosci Res Commun 28:75–84.

Kublik E (2004) Contextual impact on sensory processing at the barrel cortex of awake rat. Acta Neurobiol Exp 64:229–238.

Lee JC (1991) Morphological organization and compound action potential of sacrococcygeal dorsal roots of the rat. M.S. thesis, National Taiwan University, Taipei, Taiwan.

Mcallister JP, Willis J (1981) The structural organization of the ventral posterolateral nucleus in the rat. J Comp Neurol 197:271–301.

Moncastle VB, Henneman E (1952) The presentation of tactile sensibility in the thalamus of the monkey. J Comp Neural 97:409–439.

Paxinos G, Watson C (1998) The rat brain in stereotaxic coordinates, 4th ed. London: Academic Press.

Shaw FZ, Chen RF, Yen CT (2001) Dynamic changes of touch- and laser-evoked field potentials of primary somatosensory cortex in awake and pentobarbital-anesthetized rats. Brain Res 911:105–115.

Shyu BC, Chai SC, Kung JC, Fan RJ (2003) A quantitative method for assessing of the affective component of the pain: conditioned response associated with CO_2 laser-induced nocifensive reaction. Brain Res Protoc 12:1–9.

Woosley TA, Ven Der Loos H (1970) The structural organization of layer IV in the somatosensory region (SI) of mouse cerebral cortex. Brain Res 17:205–242.

Zhang X, Giesler GJ Jr (2005) Response characteristics of spinothalamic tract neurons that project to the posterior thalamus in rats. J Neurophysiol 93:2552–2564.

(Accepted 22 May 2008)
(Available online 1 July 2008)